ELSEVIER

Journal of Molecular Catalysis A: Chemical 193 (2003) 197–205

JOURNAL OF MOLECULAR CATALYSIS A: CHEMICAL

www.elsevier.com/locate/molcata

Adsorption of thiophene on an MoS_2 cluster model catalyst: ab initio density functional study

Hideo Orita*, Kunio Uchida, Naotsugu Itoh

Institute for Materials and Chemical Process, National Institute of Advanced Industrial Science and Technology (AIST), Tsukuba Central 5, 1-1-1 Higashi, Tsukuba, Ibaraki 305-8565, Japan

Received 24 May 2002; received in revised form 6 July 2002; accepted 25 July 2002

Abstract

Adsorption of thiophene on the coordinately unsaturated Mo atom on the $(3\,0\,\bar{3}\,0)$ plane of an $Mo_{16}S_{32}$ cluster has been investigated to develop fundamental understanding of the adsorption sites of MoS_2 catalysts in the hydrotreatment process. By using the density functional theory (DFT) method, full geometry optimization and vibrational analysis of the thiophene/cluster complex have been carried out. Adsorption energies and vibrational frequencies for different adsorption configurations have been computed. The thiophene molecule remains almost flat in the upright configuration, but becomes bent in the parallel configurations. The C–S distances become longer for all the adsorption configurations, indicating that activation of the C–S bond occurs. The C=C and C–C distances become shorter and longer for the upright configuration, respectively. For the parallel configurations, the change of distances is in the opposite direction. The most stable configuration is the bridged and rotated parallel geometry. It is easy to distinguish whether thiophene is adsorbed in the upright or parallel coordination on sulfided Mo catalysts by means of the vibrational frequencies of adsorbed thiophene. With respect to the calculated vibrational frequencies of free thiophene, the ν(C=C)asym and ν(C=C)sym bands shift to higher frequencies for the upright configuration, whereas they shift to lower for the parallel configurations.

Keywords: Density functional theory; MoS_2 catalyst model; Thiophene adsorption; Optimized configuration; Vibrational frequency

1. Introduction

In the hydrotreatment process (i.e. hydrodesulfurization (HDS) and hydrogenation (HYD)) to remove sulfur from petroleum fractions, molybdenum sulfide compounds are the important active element of the industrial catalysts. The process has recently attracted increasing interest due to new environmental legislation requiring further reduction of the sulfur content in oil products to less than 50 ppm, which leads to a need for more efficient processes and more active catalysts. A large number of experimental studies have been carried out to find the active sites on the catalyst surface and to examine the reaction mechanism involved in hydrotreatment (see reviews, e.g. [1–3]). It has now been known that properly reduced edges of molybdenum sulfide play the essential role in the reaction. However, there is no consensus on the mechanism of formation of the active sites, the exact structural configuration of the atoms constituting these sites, and the adsorption geometry of organosulfur compounds. Computational modeling techniques can provide one possible approach to get a better insight into the nature of active sites of the catalysts

* Corresponding author. Tel.: +81-298-61-4835; fax: +81-298-61-4634.
E-mail address: hideo-orita@aist.go.jp (H. Orita).

1381-1169/02/$ – see front matter © 2002 Elsevier Science B.V. All rights reserved.
PII: S1381-1169(02)00467-3

and the geometry of the adsorbate/substrate complex [4,5].

Thiophene (C_4H_4S) is the most extensively investigated as a model organosulfur compound for the HDS reaction. As the first step toward clarifying the HDS mechanism, several studies have utilized vibrational spectroscopies to investigate the adsorption of thiophene and/or CO on sulfided or nitrided Mo catalysts [6–13]. In assigning vibrational spectra of adsorbed thiophene, vibrational and/or structural data for organometallic complexes containing thiophene ligands are useful. These complexes have the great advantage that one can know from X-ray crystal data how the thiophene ligand is bound to the metal atoms. Several different bonding modes have been observed for thiophene in organometallic complexes: η^1(S)-, η^2-, η^4-, η^5-, η^4,S-μ_2-, η^4,S-μ_3-bound geometries [14]. These coordination geometries have been suggested as possible modes for thiophene adsorption on HDS catalysts. However, attention should be placed on using the data for organometallic complexes, since metal centers in organometallic complexes are not the same as sites in HDS catalysts. There are some disagreements in assigning the geometry of thiophene adsorbed on sulfided Mo catalysts. Mitchell et al. [7] have used inelastic neutron scattering (INS) and reported that thiophene is weakly chemisorbed to the catalyst surface, with 90–95% of thiophene aligned parallel with the surface (η^5-coordination) and the remaining (5–10%) adsorbed in the upright S-bound geometry (η^1(S)-coordination). Bussell and co-workers [8–10] have utilized infrared spectroscopy and concluded that thiophene is adsorbed in the upright S-bound geometry on the coordinatively unsaturated (CUS) Mo sites located at the edges of MoS_2-like structures. The reason for this disagreement is not clear, but it may be the difference in coverage of thiophene. The geometry of thiophene depends on coverage, and it is likely to change parallel to upright as the coverage increases [3].

Since it is still difficult experimentally to characterize the chemical properties of the catalyst surface and the adsorbates, many attempts at the computational simulation of the HDS reaction over metal sulfides have been made on various cluster or periodic models [15–19]. Although these studies offer some detailed insights into various properties of catalysts and adsorbates, the results of different laboratories are distinct from each other as pointed out by Ma and Schobert [18]. It is not easy to draw definite conclusions about the active sites and adsorption geometry of adsorbate. Especially, the relation between the bonding configuration of adsorbate and their vibrational spectra remains uninvestigated.

In order to simulate the surface structure of a highly dispersed MoS_2 particle, we previously chose a regular hexagonal cluster of $Mo_{27}S_{54}$ [20] because this cluster has correct stoichiometry and eletroneutrality without any saturating H atom and charge compensation as well as its size (ca. 19 Å) is comparable to that of the real catalyst particle. We have performed a full geometry optimization of the $Mo_{27}S_{54}$ cluster by using the density functional theory (DFT) method. We have found that the computed structure agrees well with the EXAFS data [21] and that the electronic properties of the atoms at various sites (i.e. corner, edge, outer, and inner positions) have been distinguished clearly by means of charge distribution and molecular orbital calculations. It is considered that the unoccupied MOs mainly move down into the band gap of the MoS_2 crystal by the formation of the peripheral edges and that the CUS Mo sites should show the stronger acceptor properties, leading to reaction with an electron donor such as thiophene in the hydrotreatment process. The edge termination of the above model seems energetically unstable compared to having several S atoms adsorbed at the Mo edge, as simulated recently by Byskov et al. [22], Raybaud et al. [23], and Schweiger et al. [24], but none of their stable configurations involve CUS Mo atoms. As there is a general agreement that the creation of CUS Mo atoms is needed for the activation of organosulfur compounds under HDS working conditions, it seems that our cluster is still useful for the model of the catalytically active surface. We have applied the previous calculational method to the adsorption of thiophene on an MoS_2 cluster model catalyst in the present work. We have computed the adsorption energies and vibrational frequencies of thiophene for different adsorption configurations, and compared our results with the experimental data of other laboratories. The computed vibrational frequencies of adsorbed thiophene are useful for assigning the geometry of thiophene adsorbed on sulfided Mo catalysts.

2. Computational methods

All the calculations were performed with the program package DMol^3 (version 4.2.1) in the Cerius^2 of Accelrys Inc. on SGI workstations of Tsukuba Advanced Computer Center (TACC) in AIST. In the DMol^3 method [25–27], the physical wave functions are expanded in terms of accurate numerical basis sets. We used the doubled numerical basis set with p-polarization function for hydrogen and d-polarization functions for other atoms (DNP), whose size is comparable to Gaussian 6–31 G**, and effective core potential (ECP) for Mo. The generalized gradient corrected (GGA) functional, by Perdew and Wang (PW91), was employed. For the numerical integration, we used the MEDIUM quality mesh size of the program. The tolerances of energy, gradient, and displacement convergence were 2×10^{-5}, 1×10^{-2}, and 1×10^{-2}, respectively. Applying symmetry conditions to reduce the computation time was not possible when ECP was used.

The crystal of MoS_2 shows a typical layered structure consisting of close-packed triangular double layers of S with each Mo atom coordinated by six S atoms in a trigonal-prismatic unit [28]. The bonding within the layers is covalent. There is only a weak van der Waal's interaction between consecutive S–Mo–S layers. Cleaving MoS_2 between the layers results in a chemically inert (0 0 0 1) surface. Geometry optimization of the MoS_2 cluster started with an initial structure with coordinates of all atoms identical to those deduced from the lattice parameters [29] of an infinite MoS_2 crystal, and the BFGS routine, in which the gradients were computed numerically, was employed. Adsorption of thiophene on the CUS Mo atom was investigated starting from different configurations. Adsorption energies were computed by subtracting the energies of the optimized gas-phase thiophene and cluster from the energy of the optimized thiophene/cluster complex as shown in Eq. (1):

$$E_{ad} = E_{thiophene/cluster} - E_{thiophene} - E_{cluster} \quad (1)$$

These adsorption energies were derived from full geometry optimizations. Therefore, they reflect any structural changes in thiophene or cluster induced by adsorption, and sometimes become a little larger than the experimental values. The conventions used here report adsorption energies as negative values in that they release heat.

Harmonic vibrational frequencies were obtained from the matrix of Cartesian second derivatives, known as the Hessian matrix, of the thiophene/cluster complex. It is not possible to compute the Hessian elements analytically in DMol^3. They are computed by displacing each atom in the model and computing a gradient vector, thus a complete second derivative matrix is built up numerically. In the present work, we calculated partial Hessian matrix including only atoms of thiophene to reduce the computation time after checking the results of the partial Hessian were almost the same as those of the full Hessian (see Table 4).

3. Results and discussion

3.1. Simplification of the $Mo_{27}S_{54}$ cluster to $Mo_{16}S_{32}$

In order to concentrate the investigation on the interaction of thiophene with the CUS Mo site of an MoS_2 cluster and reduce computationally expensive task of vibrational frequency calculations, we have simplified the previous $Mo_{27}S_{54}$ cluster to a smaller, but still stoichiometric, $Mo_{16}S_{32}$ one as shown in Fig. 1. The peripheral edges of the $Mo_{16}S_{32}$ cluster also consist of (1 0 1 0) plane (S edge) and (3 0 $\bar{3}$ 0) plane (Mo edge) only. The S atoms in the cluster can be classified into four groups according to their coordinative character: the corner and edge S atoms on ($\bar{1}$ 0 1 0) plane, the outer S atoms on (3 0 $\bar{3}$ 0) plane, and the inner S atoms, which are symbolized by $S_{c,II}$, $S_{e,II}$, $S_{o,III}$, and $S_{i,III}$, respectively. The subscripts c, e, o, and i indicate corner, edge, outer, and inner positions of the atom, respectively. Roman numeral shows the coordinative number of each Mo atom neighboring to the S atom. According to this notation, the Mo atoms also can be classified into four groups: $Mo_{c,IV}$ and $Mo_{e,IV}$ on (3 0 $\bar{3}$ 0) plane, $Mo_{o,VI}$ on ($\bar{1}$ 0 1 0) plane, and $Mo_{i,VI}$. The Mo atoms on (3 0 $\bar{3}$ 0) plane (i.e. $Mo_{c,IV}$ and $Mo_{e,IV}$) are two-fold coordinatively unsaturated sites.

First, the structural and electronic properties of the $Mo_{16}S_{32}$ cluster are compared with those of $Mo_{27}S_{54}$ to show that the simplification of the cluster size is reasonable for examining the adsorption of thiophene. Table 1 summarizes the Mo–Mo and Mo–S distances

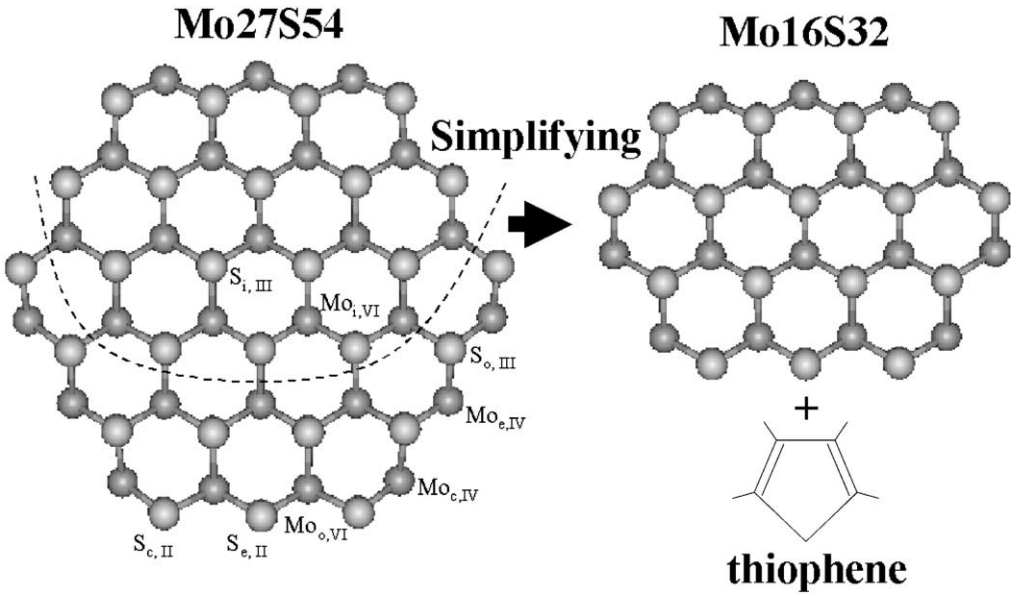

Fig. 1. Simplification of the $Mo_{27}S_{54}$ cluster to a smaller $Mo_{16}S_{32}$. The dark smaller and light larger balls in the cluster indicate Mo and S atoms, respectively. Each point corresponding to S actually represents two atoms, situated respectively in the upper and lower plane.

in the $Mo_{27}S_{54}$ and $Mo_{16}S_{32}$ cluster. The structure of the $Mo_{16}S_{32}$ cluster is also relaxed towards the edges, and two types of the Mo–Mo distances are clearly observed at the periphery. The Mo–Mo distances between the Mo atom on (3 0 $\bar{3}$ 0) and $Mo_{o,VI}$ or $Mo_{i,VI}$ are shorter (2.96–3.05 Å) than that in the crystal (3.16 Å) [29], and the distances between $Mo_{o,VI}$ and $Mo_{i,VI}$ are longer (3.22–3.32 Å) (for $Mo_{27}S_{54}$, they are 2.97–3.08 and 3.25–3.29 Å, respectively). The structure near the periphery of the $Mo_{16}S_{32}$ cluster is similar to that of $Mo_{27}S_{54}$. However, the Mo–Mo distances inside the cluster (i.e. the distances between two $Mo_{i,VI}$'s) are between 3.12 and 3.22 Å (for $Mo_{27}S_{54}$, they are 3.16–3.19 Å). They are slightly different from the Mo–Mo distance in the MoS_2 crystal, as observed previously for the smaller $Mo_{12}S_{24}$ cluster (3.27 Å) [20]. The inside of the cluster is also slightly relaxed due to its smaller size. There are edge atoms in the $Mo_{16}S_{32}$ cluster, and its relaxation is much smaller than that of $Mo_{12}S_{24}$. For the Mo–S distances in the $Mo_{16}S_{32}$ cluster, they are between 2.33 and 2.46 Å, which are the same in the $Mo_{27}S_{54}$ cluster and comparable to the Mo–S distance in the MoS_2 crystal (2.42 Å). The Mo–S distances at the periphery are shorter a little.

Table 1
Mo–Mo and Mo–S distances in the $Mo_{27}S_{54}$ and $Mo_{16}S_{32}$ cluster

	$Mo_{27}S_{54}$	$Mo_{16}S_{32}$
$Mo_{c,IV}$–$Mo_{e,IV}$	3.13	3.10
$Mo_{c,IV}$–$Mo_{c,IV}$	–	3.18
$Mo_{c,IV}$–$Mo_{o,VI}$	3.06	3.01–3.03
$Mo_{c,IV}$–$Mo_{i,VI}$	2.97	2.96–2.98
$Mo_{e,IV}$–$Mo_{i,VI}$	3.08	3.05
$Mo_{o,VI}$–$Mo_{o,VI}$	3.13	3.13
$Mo_{o,VI}$–$Mo_{i,VI}$	3.25–3.29	3.22–3.32
$Mo_{i,VI}$–$Mo_{i,VI}$	3.16–3.19	3.12–3.22
$Mo_{c,IV}$–$S_{c,II}$	2.33	2.33–2.35
$Mo_{c,IV}$–$S_{o,III}$	2.38	2.38–2.40
$Mo_{e,IV}$–$S_{o,III}$	2.38	2.39
$Mo_{o,VI}$–$S_{c,II}$	2.43	2.40–2.43
$Mo_{o,VI}$–$S_{e,II}$	2.38	2.38
$Mo_{o,VI}$–$S_{i,III}$	2.45	2.45–2.46
$Mo_{i,VI}$–$S_{o,III}$	2.46	2.43–2.46
$Mo_{i,VI}$–$S_{i,III}$	2.41–2.42	2.41–2.42

The Hirshfeld partitioned charges of the atoms in the $Mo_{27}S_{54}$ and $Mo_{16}S_{32}$ clusters are tabulated in Table 2. Mulliken charges are not used in the present work because they are very dependent on the basis sets used. The Hirshfeld partitioned charges are

Table 2
Hirshfeld partitioned charges of the atoms in the $Mo_{27}S_{54}$ and $Mo_{16}S_{32}$ cluster

Atom group	$Mo_{27}S_{54}$		$Mo_{16}S_{32}$	
	Number	Average charge	Number	Average charge
$S_{c,II}$	12	−0.177	12	−0.182
$S_{e,II}$	6	−0.168	2	−0.167
$S_{o,III}$	12	−0.130	8	−0.128
$S_{i,III}$	24	−0.107	10	−0.104
$Mo_{c,IV}$	6	0.339	6	0.339
$Mo_{e,IV}$	3	0.241	1	0.233
$Mo_{o,VI}$	6	0.291	4	0.284
$Mo_{i,VI}$	12	0.228	5	0.233

defined relative to the deformation density. The deformation density is the difference between the molecular and the unrelaxed atomic charge densities. The Hirshfeld procedure usually produces atomic charges of rather small magnitudes, but Hirshfeld charges are not so dependent on the basis sets as Mulliken ones. The outside layers of S are negatively charged, and the positively charged Mo plane is in the middle of the sandwiched structure. Highest occupied molecular orbital (HOMO) and lowest unoccupied molecular orbital (LUMO) are located at the energy value of −5.224 and −5.077 eV, respectively (for $Mo_{27}S_{54}$, they are located at −5.251 and −5.101 eV, respectively). The unoccupied MOs move down into the band gap of the MoS_2 crystal. The HOMO and LUMO of both the two clusters are populated mainly on the Mo atoms of the $(\bar{1}010)$ plane and the $(30\bar{3}0)$ plane, respectively. The structural and electronic properties of the $Mo_{16}S_{32}$ cluster correspond well to those of $Mo_{27}S_{54}$ as mentioned previously, which indicates that the simplification of the cluster size is reasonable.

3.2. Adsorption energies, structures, and vibrational frequencies of thiophene for different configurations

The adsorption of thiophene on the $Mo_{16}S_{32}$ cluster has been studied starting from different configurations. In the present work, we have limited adsorption sites of thiophene only to the Mo atoms on the $(30\bar{3}0)$ plane because it is reported that the adsorption on the S-terminated edge is always endothermic [17]. The four optimized adsorption configurations of thiophene are shown in Fig. 2A–D (for top view, lower part of the $Mo_{16}S_{32}$ cluster is cut and only part of the $(30\bar{3}0)$ plain is shown). The thiophene molecules in configuration A and others are bound to the cluster in the upright and parallel geometries, respectively. Thiophene remains almost flat in configuration A, but becomes bent in other configurations to reduce the geometrical restriction from the Mo atoms in the cluster. The bonding modes in the present cluster are somewhat different from those reported in organometallic complexes [14]. We could not obtain any stable adsorption configuration in η^5-bound geometry even when a η^5-bound structure was used as initial starting geometry.

The computed results (adsorption energies and distances between atoms) as well as the experimental data for thiophene are tabulated in Table 3. The most stable configuration is not C (the optimized structure of C has two imaginary vibrational frequencies in the full Hessian vibrational calculation, and corresponds to a higher-order saddle point on the potential energy surfaces rather than a local minimum), but D. The geometry and adsorption energy for C are similar to those reported by Raybaud et al. [17] in their periodic model simulation. In configuration D, the thiophene molecule is rotating from configuration C, and

Table 3
Adsorption energies and distances between atoms for free and adsorbed thiophene

	C_4H_4S (experimental)[a]	C_4H_4S (calculated)	η^1(S) (A)	η^2 (B)	η^4,S-μ_2 (C)	η^2-S,C and η^2-C (D)
E_{ad} (eV)			−1.11	−0.79	−1.81	−2.72
D(C–S) (Å)	1.71	1.73	1.75	1.82	1.82	1.82, 1.85
D(C=C) (Å)	1.37	1.37	1.36	1.44, 1.45	1.42	1.44, 1.49
D(C–C) (Å)	1.42	1.42	1.44	1.39	1.41	1.40
D(Mo–S)first (Å)			2.35	2.97	2.65	2.20
D(Mo–S)second (Å)			4.02	4.28	3.10	3.35

[a] [14].

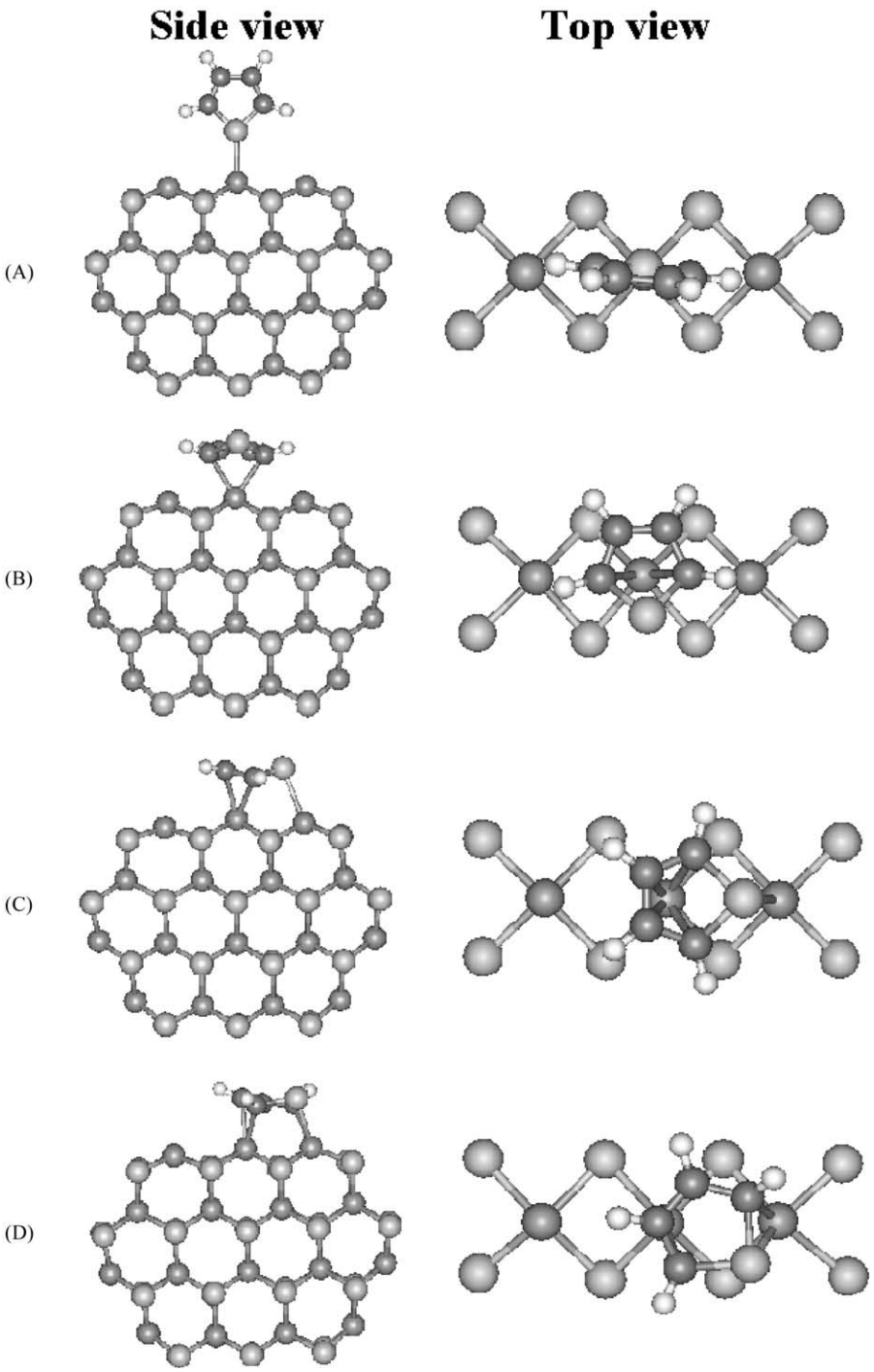

Fig. 2. Optimized adsorption configurations of thiophene on the $Mo_{16}S_{32}$ cluster. For top view, the lower part of the $Mo_{16}S_{32}$ cluster is cut and only part of the $(3\,0\,\bar{3}\,0)$ plain is shown.

becomes closest and almost parallel to the $(3\,0\,\bar{3}\,0)$ plain. The right side of the cluster structure in configuration D is slightly disturbed. The configuration B shows the smallest adsorption energy, and the S atom of thiophene does not interact directly with the Mo atoms in the cluster (the shortest and second shortest Mo–S distances (D(Mo–S)first and D(Mo–S)second) are 2.97 and 4.28 Å, respectively). This configuration may represent a weakly chemisorbed precursor state as suggested by Mitchell et al. [7]. The geometry and adsorption energy of configuration A are almost the same as those for the upright S-bound coordination reported by Raybaud et al. [17]. The thiophene is tilted a little in configuration A (this structure has one imaginary frequency in the full Hessian vibrational calculation, and corresponds to a transition state on the potential energy surfaces). When compared to free thiophene, the C–S distances become longer for all the adsorption configurations, indicating that activation of the C–S bond occurs. The C=C and C–C distances become shorter and longer for the upright configuration, respectively. For the parallel configurations, the change of distances is in the opposite direction.

The bonding modes can be distinguished clearly by vibrational frequencies of adsorbed thiophene. Table 4 shows the computed vibrational frequencies for free and adsorbed thiophene as well as the experimental data [30]. We have followed the notation of mode assignments in [10]. Relative shift in the last column of Table 4 indicates significant shifts from the calculated frequencies of free thiophene (shifts to higher and lower frequencies are indicated by + and −, respectively). For some adsorption configurations, we have calculated full Hessian matrix including all the atoms in thiophene/cluster complex. All the frequencies except two modes in configuration C equal within 3 cm^{-1}, which shows the partial Hessian calculation gives quite good results. With respect to the calculated vibrational frequencies of free thiophene, the ν(C=C)asym and ν(C=C)sym bands shift to higher frequencies for the upright configuration, whereas they shift to lower for the parallel configurations. This frequency change is consistent with the experimental results of organometallic complexes reported by Mills et al. [10]. The frequency of the #8 ν(ring) mode becomes lower for the parallel configurations than the upright one. As regards the #15 δ(ring)defm, ν(CS)asym, and #19 δ(ring)defm modes, in which the contribution of the C–S stretching is definite, their frequencies become much lower for the parallel configurations than the upright one. The frequency of the out-of-plain #17 ρwag(CH) mode becomes higher for the parallel configurations than the upright one, which is also consistent with the spectra of INS [7] and IR [10] for organometallic complexes.

Tarbuck et al. have measured the IR spectrum for thiophene adsorbed on the sulfided Mo catalyst, and found a new peak located at 1430 cm^{-1} [8]. They have assigned this peak as the ν(C=C)sym mode of thiophene adsorbed in an upright geometry on the CUS Mo sites located at the edges of MoS_2-like structures. They did not observe any shift or shoulder of the strong peak at 1252 cm^{-1} (#8 ν(ring) mode). The results presented here support their assignment of the bonding geometry of thiophene. For the upright geometry, the ν(C=C)sym mode shifts to higher frequency and the #8 ν(ring) mode shifts little, whereas the ν(C=C)sym and #8 ν(ring) modes shift to lower frequency definitely for the parallel geometries. The IR spectra are unfortunately restricted to the region above 1000 cm^{-1} because of strong absorption of the oxide catalyst support. It would be possible to make the assignment more definite by using our results if a spectrum below 1000 cm^{-1} is measured together by other methods such as INS, Raman, and inelastic electron tunneling spectroscopies. The INS spectra of adsorbed thiophene of Mitchell et al. [7] look more like the spectrum of pure thiophene than coordinated one, which is also coincident with our results. It seems probable that thiophene is adsorbed on sites other than the CUS Mo atoms in their catalyst. Therefore, the vibrational calculation of thiophene/cluster complex is useful for assigning the geometry of thiophene adsorbed on sulfided Mo catalysts. It is worth discussing as to why Bussell et al. did not observe a parallel configuration. The configurations of C and D, which are more stable than the upright configuration of A, need two neighboring CUS Mo sites. As pointed out already by Mitchell et al. [7], the pretreatment conditions of Bussell et al. are mild, and smaller amounts of CUS Mo sites are produced on their catalyst. Probably there are few two neighboring CUS Mo sites, which are suitable for the parallel coordination of thiophene, on their catalyst.

Table 4
Vibrational frequencies (in cm^{-1}) for free and adsorbed thiophene

No.	Assignment[a]	C_4H_4S (experimental)[b]	C_4H_4S (calculated)	η^1(S) (A)		η^2 (B)	η^4,S-μ_2 (C)		η^2-S,C and η^2-C (D)	Relative shift	
				Partial	Full		Partial	Full		Upright	Parallel
1	ν(CH)	3126	3223	3219	3219	3241	3210	3209	3203		
2	ν(CH)	(3125)	3209	3208	3207	3184	3188	3188	3187		
3	ν(CH)	3098	3172	3191	3191	3113	3176	3176	3137		
4	ν(CH)	3098	3171	3179	3179	3059	3164	3166	3086		
5	ν(C=C)asym	1507	1485	1530	1531	1451	1376	1375	1334	+	−
6	ν(C=C)sym	1409	1343	1423	1432	1222	1274	1273	1209	+ +	− −
7	ν(ring)	1360	1395	1328	1327	1352	1401	1401	1437		
8	ν(ring)	1256	1237	1217	1218	1161	1194	1194	1181	−	− −
9	δ(CH)asym	(1085)	1071	1065	1065	989	1040	1040	1026		
10	δ(CH)sym	1083	1073	1061	1060	1008	1061	1062	1075		
11	ν(ring)	1036	1029	1009	1008	1085	1044	1045	948		
12	ρwag(CH)	898	886	910	911	915	886	885	878		
13	δ(ring)defm	872	852	862	862	880	825	825	798		
14	ρwag(CH)	867	840	889	889	836	832	831	864		
15	δ(ring)defm	839	827	786	786	653	736	735	681	−	− −
16	ν(CS)asym	751	739	681	681	603	599	600	597	−	− −
17	ρwag(CH)	712	691	733	734	802	794	785	760	+	+ +
18	ρwag(CH)(sh)	683	636	700	700	716	764	764	712	+	+
19	δ(ring)defm	608	607	604	604	506	509	507	498	δ −	− −
20	τ(ring)	565	545	530	529	532	543	544	548		
21	τ(ring)	452	444	412	409	414	421	426	454		

[a] [10].
[b] [27].

4. Conclusions

Adsorption of thiophene on an MoS_2 cluster model catalyst has been investigated to develop a fundamental understanding of the adsorption sites of MoS_2 catalysts in the hydrotreatment process. First, the $Mo_{27}S_{54}$ cluster, which was investigated previously, has been simplified to a smaller, but still stoichiometric, $Mo_{16}S_{32}$ one. The structural and electronic properties of the $Mo_{16}S_{32}$ cluster are found to correspond well to those of $Mo_{27}S_{54}$, showing that the simplification of the cluster size is reasonable.

Full geometry optimization and vibrational analysis of the thiophene/cluster complex have been carried out. Thiophene is adsorbed on the edge Mo atom on the $(3\,0\,\bar{3}\,0)$ plane to represent the adsorption on the CUS Mo atom of sulfided Mo catalysts. Adsorption energies and vibrational frequencies for different adsorption configurations have been computed. The thiophene molecule remains almost flat in the upright configuration, but becomes bent in the parallel configurations. The C–S distances become longer for all the adsorption configurations, indicating that activation of the C–S bond occurs. The C=C and C–C distances become shorter and longer for the upright configuration, respectively. For the parallel configurations, the change of distances is in the opposite direction. The most stable configuration is the bridged and rotated parallel geometry, which becomes closest and almost parallel to the $(3\,0\,\bar{3}\,0)$ plain as shown in Fig. 2D.

The computed vibrational frequencies of adsorbed thiophene are useful for assigning the geometry of thiophene adsorbed on sulfided Mo catalysts. It is easy to distinguish whether thiophene is adsorbed in the upright or parallel coordination by means of vibrational frequencies of adsorbed thiophene. For example, the ν(C=C)asym and ν(C=C)sym mode shift to higher frequency and the #8 ν(ring) mode shifts little for the upright geometry, whereas all the above three modes shift to lower frequency definitely for the parallel geometries. The frequency of the out-of-plain #17 ρwag(CH) mode becomes much larger for the parallel configurations than the upright one.

References

[1] A.N. Startsev, Catal. Rev. Sci. Eng. 37 (1995) 353.
[2] S. Eijsbouts, Appl. Catal. A 158 (1997) 53.
[3] B.C. Wiegand, C.M. Friend, Chem. Rev. 92 (1992) 491.
[4] R.A. van Santen, M. Neurock, Catal. Rev. Sci. Eng. 37 (1995) 557.
[5] J.W. Andzelm, A.E. Alvarado-Swaisgood, F.U. Axe, M.W. Doyle, G. Fitzgerald, C.M. Freeman, A.M. Gorman, J.-R. Hill, C.M. Kölmel, S.M. Levine, P.W. Saxe, K. Stark, L. Subramanian, M.A. van Daelen, E. Wimmer, J.M. Newsam, Catal. Today 50 (1999) 451.
[6] E. Diemann, Th. Weber, A. Mülller, J. Catal. 148 (1994) 288.
[7] P.C.H. Mitchell, D.A. Green, E. Payen, J. Tomkinson, S.F. Parker, Phys. Chem. Chem. Phys. 1 (1999) 3357.
[8] T.L. Tarbuck, K.R. McCrea, J.W. Logan, J.L. Heiser, M.E. Bussell, J. Phys. Chem. B 102 (1998) 7845.
[9] P. Mills, D.C. Phillips, B.P. Woodruff, R. Main, M.E. Bussell, J. Phys. Chem. B 104 (2000) 3237.
[10] P. Mills, S. Korlann, M.E. Bussell, M.A. Reynolds, M.V. Ovchinnikov, R.J. Angelici, C. Stinner, T. Weber, R. Prins, J. Phys. Chem. A 105 (2001) 4418.
[11] A. Travert, C. Dujardin, F. Mauge, S. Cristol, J.F. Paul, E. Payen, D. Bougeard, Catal. Today 70 (2001) 255.
[12] F. Mauge, J. Lamotte, N.S. Nesterenko, O. Manoilova, A.A. Tsyganenko, Catal. Today 70 (2001) 271.
[13] Z. Wu, C. Li, Z. Wei, P. Ying, Q. Xin, J. Phys. Chem. B 106 (2002) 979.
[14] R.J. Angelici, Coord. Chem. Rev. 105 (1990) 61.
[15] M. Neurock, R.A. van Santen, J. Am. Chem. Soc. 116 (1994) 4427.
[16] J.A. Rodriguez, J. Phys. Chem. B 101 (1997) 7524.
[17] P. Raybaud, J. Hafner, G. Kresse, H. Toulhoat, Phys. Rev. Lett. 80 (1998) 1481.
[18] X. Ma, H.H. Schobert, J. Mol. Catal. A 160 (2000) 409.
[19] V. Alexiev, R. Prins, T. Weber, Phys. Chem. Chem. Phys. 3 (2001) 5326.
[20] H. Orita, K. Uchida, N. Itoh, J. Mol. Catal. A, in press.
[21] C. Calais, N. Matsubayashi, C. Geantet, Y. Yoshimura, H. Shimada, A. Nishijima, M. Lacroix, M. Breysse, J. Catal. 174 (1998) 130.
[22] L.S. Byskov, J.K. Nørskov, B.S. Clausen, H. Topsøe, J. Catal. 187 (1999) 109;
L.S. Byskov, J.K. Nørskov, B.S. Clausen, H. Topsøe, Catal. Lett. 64 (2000) 95.
[23] P. Raybaud, J. Hafner, G. Kresse, S. Kasztelan, H. Toulhoat, J. Catal. 189 (2000) 129;
P. Raybaud, J. Hafner, G. Kresse, S. Kasztelan, H. Toulhoat, J. Catal. 190 (2000) 128.
[24] H. Schweiger, P. Raybaud, G. Kresse, H. Toulhoat, J. Catal. 207 (2002) 76.
[25] B. Delley, J. Chem. Phys. 92 (1990) 508.
[26] B. Delley, J. Phys. Chem. 100 (1996) 6107.
[27] B. Delley, J. Chem. Phys. 113 (2000) 7756.
[28] P. Raybaud, G. Kresse, J. Hafner, H. Toulhoat, J. Phys. Condens. Mat. 9 (1997) 11085, 11107.
[29] K.D. Bronsema, J.L. de Boer, F. Jellinek, Z. Anorg. Allg. Chem. 540/541 (1986) 15.
[30] M. Rico, J.M. Orza, J. Morcillo, Spectrochim. Acta 21 (1965) 689.